Geophys. J. Int. (1993) **114**, 325–340

Origins of amplitude variations in seismic doublets: source or attenuation process?

Jean-Luc Got and Julien Fréchet

Laboratoire de Géophysique Interne et Tectonophysique, IRIGM, BP 53X, 38041 Grenoble Cedex, France

Accepted 1993 January 7. Received 1993 January 7; in original form 1991 October 18

SUMMARY

Accurate estimates of spectral ratios of two doublets (i.e. similar seismic events) occurring along the San Andreas Fault, in the Hollister region have been computed using a cross-spectral method.

Both events of each doublet occurred within a 24 hr interval. Although both waveforms of a doublet are remarkably similar, computed spectral ratios exhibit strong, but steady variations with frequency in the first arrivals. The attenuation process can explain neither the sign nor the order of magnitude of these variations. On the contrary, they are closely related to the source mechanism: we show that the slope computed from the linear and coherent part of the spectral ratio is an estimation of the variation in the apparent rupture duration between the two events. One doublet exhibits an azimuthal distribution of the spectral-ratio variations that is interpreted as the result of a change in the position of the hypocentres, relative to the rupture area. For this doublet, location of hypocentres varies only from 10 to 30 per cent of the source length: this points out that small changes in rupture kinematics can lead to significant variations in the spectral ratio of earthquake doublets, i.e. in the amplitude of each event. For the other doublet, the variations are related to a change in source length.

We also have computed spectral ratios all along the seismograms, using a moving window technique. When an azimuthal distribution of the spectral ratio is observed in the first arrivals, we notice a decrease of the spectral ratio all along the seismograms. The doublet with strong, but non-azimuthal variations of the spectral ratio in the first arrivals, does not indicate such a decrease of the spectral ratio along the seismogram. This implies that the variations of the coda decay are related not only to temporal or spatial changes of attenuation but also to source parameters. These variations have the same order of magnitude as those provoked by a temporal change in coda Q of 10 per cent. They can occult time changes of spectral ratio, for instance in case the attenuation in the crust would vary before a strong earthquake.

Key words: attenuation, coda, doublet, seismic source, spectral ratio.

INTRODUCTION

Numerous studies (Chouet 1979; Aki 1985; Gusev & Lemzikov 1985; Novelo-Casanova *et al.* 1985; Sato 1986; Jin & Aki 1986; Peng *et al.* 1987; see Sato 1988; Jin & Aki 1989 and Frankel 1991 for reviews) have dealt with the determination of changes of crustal properties (seismic velocities, attenuation) before major earthquakes. A large part of these papers are interested in temporal variations in coda Q of microearthquakes. They often reveal that patterns of temporal changes in Q^{-1} are complex and very different. More recently, Peacock *et al.* (1988), Crampin *et al.* (1990) have reported evidences for changes in shear wave splitting at Anza before the North Palm Springs earthquake. Both coda Q and shear wave splitting studies are based on statistical analysis of large sets of seismic events. However, it is difficult from these studies to discard unambiguously the possibility of spatial variations due to different distributions of data sets. To avoid such spatial variations, Poupinet, Ellsworth & Fréchet (1984), Fréchet (1985) and recently Aster, Shearer & Berger (1990) have used microearthquake doublets (close-by events with similar waveforms) to

measure accurately seismic velocity changes. The present work has been initiated in order to measure temporal variations of attenuation in the crust before earthquakes of large magnitudes, using microearthquake doublets. Frémont & Poupinet (1987) have used spectral ratios in body waves of doublets to measure such variations. To eliminate the effects of possible source changes, Got, Poupinet & Fréchet (1990) have investigated spectral ratios in coda waves of doublets. However, a preliminary study of spatial doublets (doublets for which the two events occur in a very short lapse of time) has shown that there were, even in their coda, amplitude changes which can not be due to temporal coda-Q variations. In this paper, we are interested in understanding the origin of these amplitude changes, using a spectral-ratio method.

ANALYSIS OF THE DATA

Estimation of the spectral ratio

The spectral ratio is defined as the module of the transfer function $G(f)$ relating the Fourier transforms of two signals $x(t)$ and $y(t)$. The estimation is performed for adjacent windows of the signal using the moving window technique (Poupinet *et al.* 1984; Fréchet 1985) and the classical cross-spectral method (Jenkins & Watts 1968).

We compute the least-squares estimate $\hat{G}(f)$ of $G(f)$ as:

$$\hat{G}(f) = \frac{\overline{X(f)Y^*(f)}}{\overline{Y(f)Y^*(f)}} \tag{1}$$

where $X(f)$ and $Y(f)$ are the Fourier transforms of $x(t)$ and $y(t)$. The star denotes complex conjugate, and the overbar indicates smoothed values. The smoothing function of the spectral densities is the Fourier transform of a Tukey window of order two.

Approximate $100(1-\alpha)$ per cent confidence intervals for $\hat{G}(f)$ are (Jenkins & Watts 1968):

$$\hat{G}(f)\left[1 \pm \left(\frac{2}{\nu-2} F_{2\nu-2}(1-\alpha)\frac{1-C^2(f)}{C^2(f)}\right)^{1/2}\right] \tag{2}$$

where $C(f)$ is the coherency,

$$\nu = \frac{\left[\sum_{k=-N}^{k=N} l(k)\right]^2}{\sum_{k=-N}^{k=N} l^2(k)}$$ is the number of degrees of freedom,

and $l(k)$, $-N \le k \le N$, is the smoothing function. $G(f)$ is assumed to follow approximately a Fisher distribution with 2 and $\nu - 2$ degrees of freedom. Let Z be a random variable of mean μ and variance σ which follows such a distribution; the function $F_{2,\nu-2}(1-\alpha)$ is defined by

$$\text{Prob}\left[\frac{|Z-\mu|}{\sigma} \le F_{2,\nu-2}(1-\alpha)\right] = 1-\alpha.$$

The confidence intervals narrow as the number of degrees of freedom (i.e. the smoothing) or the coherency increases.

Estimation of the coherency

The coherency is estimated by:

$$\hat{C}(f) = \frac{\overline{X(f)Y^*(f)}}{\sqrt{\overline{X(f)X^*(f)}}\sqrt{\overline{Y(f)Y^*(f)}}}. \tag{3}$$

The coherency, which varies in the interval $[0, 1]$, allows the evaluation of the linearity and the stationarity of the relation between $X(f)$ and $Y(f)$, as well as the level of the signal-to-noise ratio.

The distribution of the coherency estimate is not a simple distribution; in order to compute the confidence interval on the coherency, we use the Fisher's z transformation

$$z = \tanh^{-1}[\hat{C}(f)]$$
$$= \frac{1}{2}\ln\frac{1+C(f)}{1-C(f)}$$

the parameter z follows approximately a Gaussian distribution of mean μ and variance $\sigma^2 = 1/B_w T$ where B_w is the equivalent bandwidth of the smoothing function and T the sampling period. Let us define η using the relation:

$$\text{Prob}\left[\frac{|z-\mu|}{\sigma} \le \eta\left(1-\frac{\alpha}{2}\right)\right] = 1-\alpha.$$

The $100(1-\alpha)$ per cent confidence interval for z is $\mu \pm \eta(1-(\alpha/2)/\sqrt{B_w T}$. Consequently, the $100(1-\alpha)$ per cent confidence interval for the coherency is:

$$I_c = \left\{\tanh\left[z - \eta\left(1-\frac{\alpha}{2}\right)\Big/\sqrt{B_w T}\right],\right.$$
$$\left.\tanh\left[z + \eta\left(1-\frac{\alpha}{2}\right)\Big/\sqrt{B_w T}\right]\right\}. \tag{4}$$

This confidence interval is not centred on $\hat{C}(f)$.

Effect of noise on the estimation of spectral ratio

Spectral ratios, even estimated as in (1), are strongly affected by noise. However, spectral ratio fluctuations are directly related to coherency drops. There is nothing surprising about that, since the coherency can be written as the geometric mean of the transfer functions

$$\hat{G}_{XY}(f) = \frac{\overline{X(f)Y^*(f)}}{\overline{Y(f)Y^*(f)}} \quad \text{and} \quad \hat{G}_{YX}(f) = \frac{\overline{X(f)Y^*(f)}}{\overline{X(f)X^*(f)}},$$

whose modules are the estimates of the spectral ratios of $x(t)$ relative to $y(t)$ and conversely. The coherency is therefore the appropriate tool to weight adjustments or averages, to minimize the influence of noise on the estimation of spectral ratio variations. In the following adjustments and averages, we will use a weight inversely proportional to the variance of $\ln G(f)$, for coherencies greater than 0.90:

$$\begin{cases} w^2 = \dfrac{C^2}{1-C^2} & 0.9 \le C < 1. \\ = 0. & 0. \le C < 0.9. \end{cases} \tag{5}$$

Relations (2) and (4) show that when $C(f)$ is lower than 0.90, both $G(f)$ and $C(f)$ are poorly estimated.

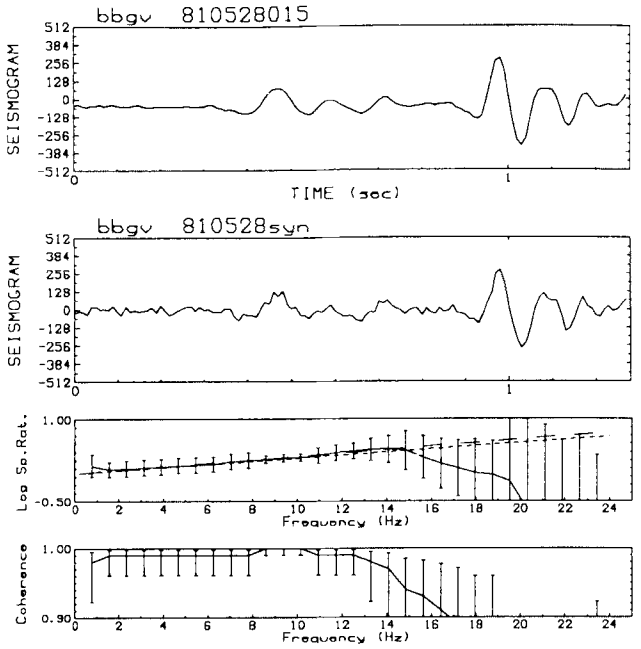

Figure 1. Seismograms, logarithm of spectral ratio and coherency computed for the doublet constituted from the two signals $s_1(t)$ and $s_2(t)$ (see text). White noise has a maximum absolute value of 50. Vertical bars represent 90 per cent confidence intervals for logarithm of spectral ratio and coherency. Dashed line indicates the expected spectral ratio. Dotted line corresponds to the estimated average variation of the spectral ratio.

This weighting function allows reliable estimates of spectral ratio variations. We will illustrate this purpose by altering an initial seismic signal $s_1(t)$ in a signal $s_2(t)$, by the mean of Fourier transforms:

$$s_2(t) = \mathrm{FFT}^{-1}\{\exp(-\alpha f)\,\mathrm{FFT}[s_1(t)]\} + n(t)$$

where α is the parameter we adjust, f is the frequency, and $n(t)$ is a white noise. Fig. 1 displays signals, cross spectrum, spectral ratio and coherency for one window of both signals. It appears that computed spectral ratios are close to the model (dashed line) until coherence severely decreases. A weighted linear adjustment of $\ln G(f)$ [using the weight (5)] leads to an estimation of α with a relative error of less than 5 per cent.

Presentation of the data set and processing

The data used in this study were collected from the CALNET array, located along the San Andreas and Calaveras Faults in Central California (Fig. 2). Possible doublets were selected from an earthquake catalogue of well-located events for the years 1978–1982, according to a distance criterion (Poupinet *et al.* 1984). Up to 150 earthquakes were digitized. Among them, 67 events appeared to belong to 24 doublets or multiplets. From this data set, we selected the best two spatial doublets with an inter-event distance smaller than 100 m (Table 1). Both doublets exhibit a coherency high enough to allow the estimation of spectral ratios. Their locations are shown on Fig. 2, and their parameters are listed in Table 1. The first 30 s of each seismogram were digitized at a rate of 100

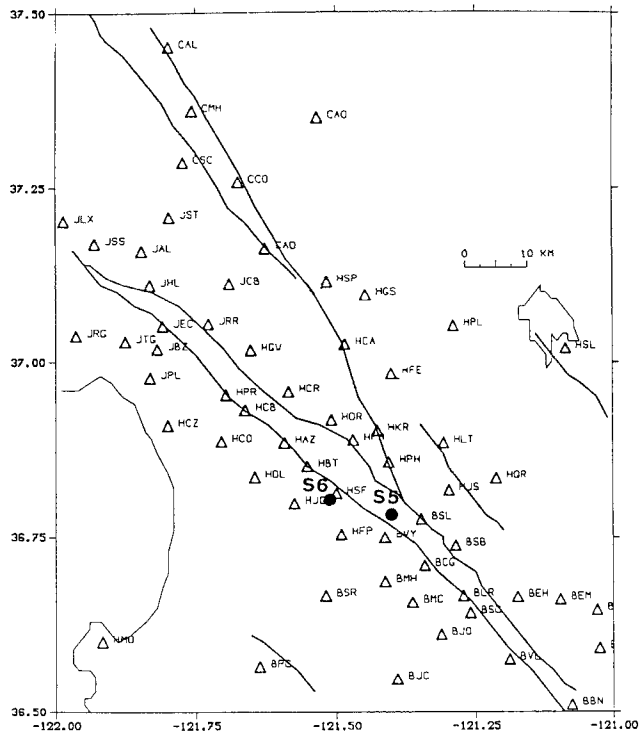

Figure 2. Map of Central California showing CALNET stations (triangles) and absolute locations of doublets studied (circles).

samples/s. No change of digitization channel has been reported during the period (less than one day) covered by each doublet. The processing was performed using a 1.28 s long time window, with cosine taper, which moves along the seismograms at steps of 0.25 s. To have a minimum bias on the estimation of $G(f)$ and $C(f)$, the time delay between the two signals is computed and the time windows are aligned to the nearest sample at each step. A short time window was chosen because of the non-stationary character of the signals. A longer window would have included different seismic arrivals. In order to be able to observe rapid variations in the frequency content, a narrow smoothing function defined as a five-point operator, and corresponding to a low $B_w T$ value was used. The disadvantage of such small widths is that confidence intervals are large and strongly dependent on the coherency.

We compute spectra of the two events, spectral ratio and coherency over a broad (1–25 Hz) frequency range. We also compute, using the weight defined in (5), the weighted geometric mean of the spectral ratio in the low frequency band 3–8 Hz over the whole set of stations, which we call $\bar{G}_{LFm}$.

Table 1. Location, date, magnitude and relative relocations (Fréchet 1985) of the events selected; $X>0$ East, $Y>0$ North, $Z>0$ Down, d: inter-event distance.

Doublet	UID	Lat.N.	Long.W.	Depth (km)	Magn.	X(m)	Y(m)	Z(m)	d(m)
S5	810528015	36 46.99	121 24.05	8.09	1.8	0.	0.	0.	77
	810528016	36 46.99	121 23.94	8.08	1.6	-5.	40.	-66.	
S6	811128005	36 48.23	121 30.73	5.02	1.7	0.	0.	0.	70
	811128013	36 48.24	121 30.66	5.16	1.6	43.	-49.	11.	

RESULTS

Fig. 3 shows a set of spectra, spectral ratios and coherency for P waves of the two doublets, recorded on the vertical component of several stations. The spectrum of each event of a doublet is plotted on the top. These velocity spectra are uncorrected for the instrument responses, which are identical for both events. Both spectra are normalized with respect to their respective maximum values. The solid line corresponds to the first event and the dotted line to the second. The spectral ratio and the estimated errors are presented in the middle of each figure on a logarithmic scale. The coherency is presented at the bottom of each figure: notice that the vertical scale is between 0.9 and 1.0. For each doublet, a plot of the mean slope of the spectral ratio is displayed versus aximuth (bottom set of figures).

An ideal doublet is one which is made up of two identical events. On this case the spectra are the same and the spectral ratio is equal to one throughout the entire frequency band. Instead, we observe that:

—the spectra are not exactly identical;

—the mean of the spectral ratio is not equal to one;

—the spectral ratio $G(f)$ varies over the frequency band 1–25 Hz.

The mean $\bar{G}_{LFm}$ of the spectral ratio in the low-frequency band over the whole set of stations is 0.91 for the S6 doublet, 1.84 for the S5 one. This shows that both events of the S6 doublet have about the same mean amplitude (i.e. the same seismic moment). On the other hand, the mean amplitude ratio of the S6 doublet reaches a value close to 2.

(a) S6 doublet

Spectra are very similar over the frequency band 1–255 Hz. Two kinds of variation appear, which are not mutually exclusive (Fig. 3):

—a frequency shift;

—changes of the spectral shape.

Stations recording the S6 doublet (Fig. 3a), especially HGS, JRR and HGW show clear examples of frequency shifts. Note that for stations HGS and JRR the spectra are strikingly similar, except that one of the spectra (dotted line) is shifted towards the low frequencies relative to the other. However, the frequency shifts are not easy to compute with accuracy, for the whole set of stations.

The spectral ratio is not constant throughout the whole frequency range. Its variation is regular in the frequency band where the coherency is greater than 0.9. The linear trend is not an effect of smoothing, which is kept light ($\nu = B_w T \approx 4$). On the contrary, this trend emphasizes the absence of systematic strong variations in large frequency bands. As the variations of $\ln G(f)$ are weak and approximately linear, a weighted linear adjustment has been performed using the weight defined by (5). We call a the slope computed from $\ln G(f)$. a has the dimension of a time. As will be discussed further, the unusual linearity of spectral ratios with frequency is directly related to the weak shifts between the spectra. Although it is difficult to estimate these frequency shifts with accuracy, Fig. 3 qualitatively shows the (inverse) correlation between frequency shifts and a slopes.

The a slopes have been plotted as a function of azimuth (Fig. 3a, bottom). The S6 doublet shows a clear azimuthal variation of the a slopes. They have a negative minimum for the stations situated southeast of the doublet, and a positive maximum for those situated northwest (i.e. remarkably along the N340 direction of the San Andreas Fault). Notice that the signs of the slopes are opposite for opposite azimuths relative to the epicentre. The poor determination and the narrow range of incidence angles (Table 2) does not allow to point out a relation between a slope and incidence angle.

(b) S5 doublet

The spectra of this doublet exhibit important variations (Fig. 3b). It is difficult to distinguish frequency shifts from changes in spectral shapes. However, the dominant frequency of the second event (dotted line) is higher than that of the first one (solid line), regardless of the station. This difference displays a negative correlation with the spectral-ratio slope.

Variations of the spectral ratio are stronger and the coherency lower for this doublet (Fig. 3b) than for the S6 doublet (note change in ordinates at the bottom of Fig. 3b). Linear regression gives a slopes (and confidence intervals on these slopes) twice as high as those of S6. Although second-order variations are present, we notice that these slopes are negative for all the stations.

DISCUSSION

As it has been outlined in introduction, our original centre of interest is the study of coda-Q^{-1} changes related to the occurrence of a major earthquake, using temporal doublets of micro-earthquakes. This idea has led us to investigate at first the coda of spatial doublets, for which temporal variations of Q^{-1} are thought to be null. However, various kinds of changes are observed, tending to suggest that time changes of coda amplitudes are not independent from frequency variations in first arrivals. In the following paragraphs, we attempt to discuss completely the origin of the changes reported, in the first arrivals as well as in the coda waves.

Since the time elapse between the two events of a spatial doublet is very short, it is unlikely that a change in the frequency response of the stations can take place. The spectral-ratio variations can hence be attributed, either to the propagating medium, or to the source of the events.

Effects of the propagating medium

Let us first make the assumption that the spectral variations observed are due to the propagating medium in the vicinity of the source. The short time elapse between the occurrences of the two events allows us to ignore any temporal variations of the crust outside the source region.

As the two events of a doublet are very closely located, the ray paths between source and receiver are practically identical. The change in spectral ratio can be due either to the attenuation between the two hypocentres, or to a variation of attenuation related to the occurrence of the first earthquake. We investigate these two effects in the following discussion.

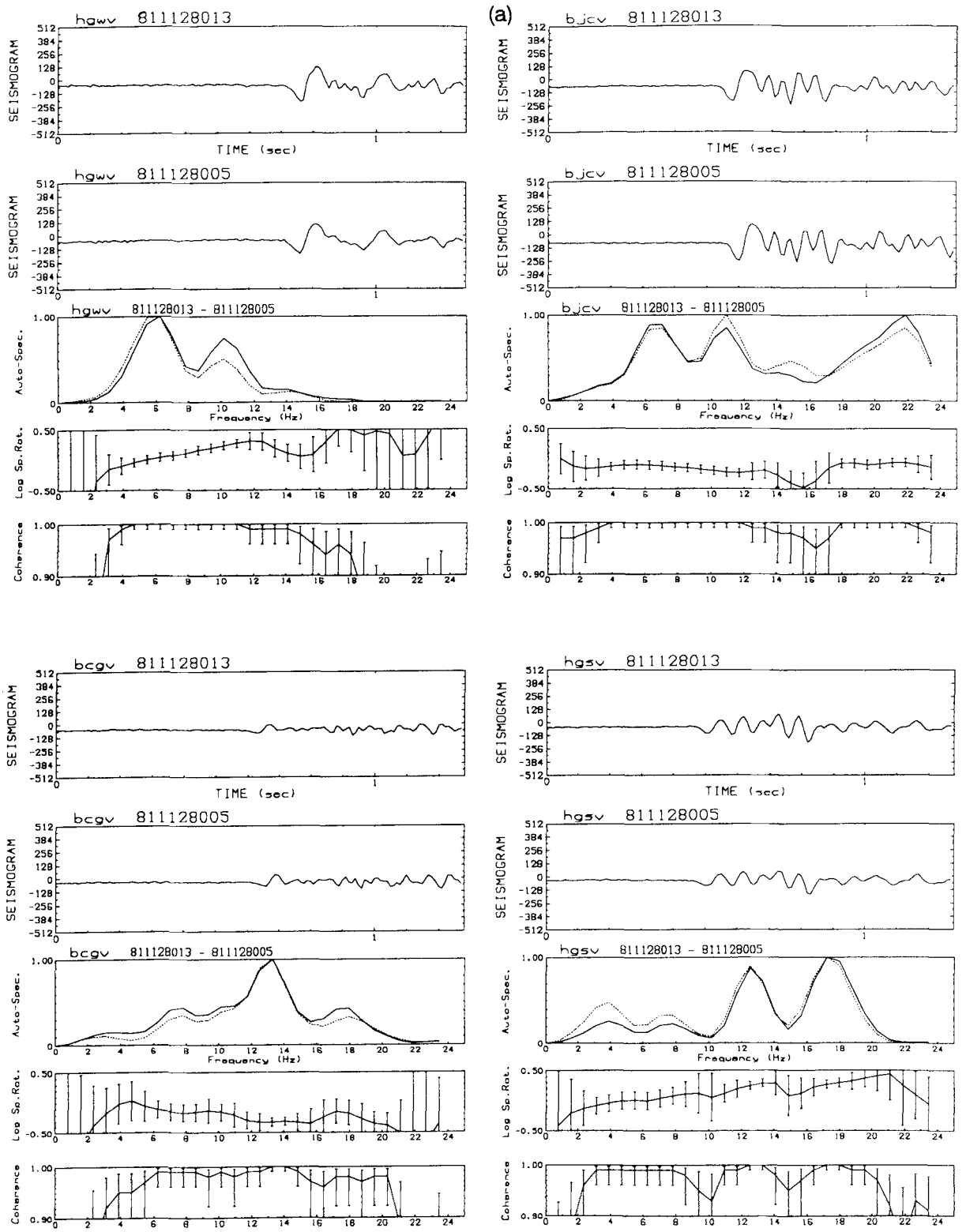

Figure 3. Seismograms, auto-spectra, logarithm of spectral ratio and coherency in the *P* waves for the S6 (a) and S5 (b) doublets. Each auto-spectrum is a velocity spectrum normalized relative to its own maximum. Dotted line indicates the spectrum of the second event. Vertical bars represent 90 per cent confidence intervals for logarithm of spectral ratio and coherency. Bottom: slopes of *P*-waves spectral-ratio logarithm $\times 100$ as a function of azimuth for S6 and S5 doublets. Triangles indicate different stations. Vertical bars represent confidence intervals.

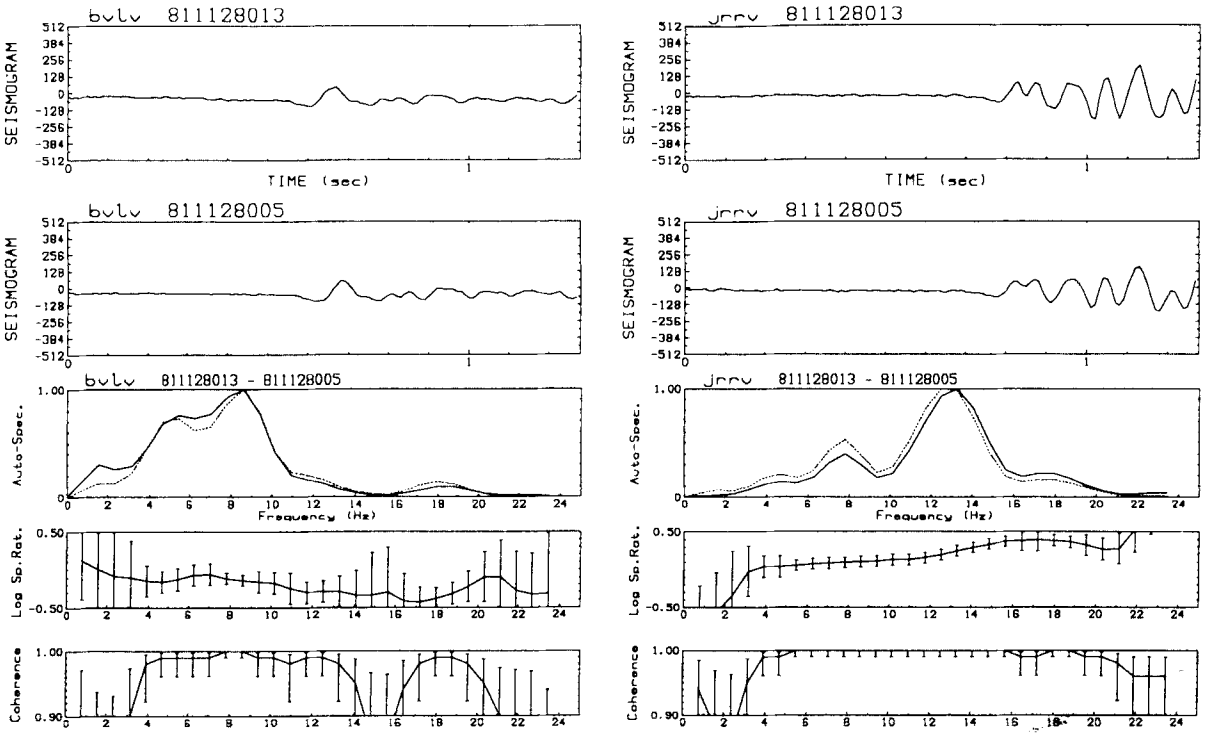

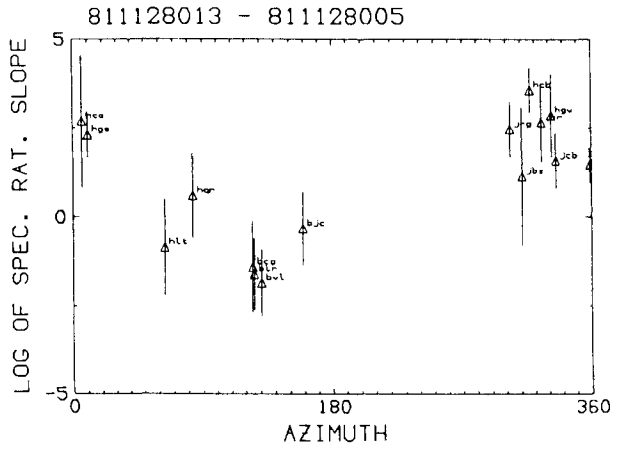

Figure 3(a). (*Continued.*)

(a) Attenuation between the two hypocentres

Let us consider the S6 doublet. Fig. 4 shows a sketch of the two hypocentres using the relative relocations of Fréchet (1985) (Table 1). We observe that the stations located NW of the doublet show a positive slope, whereas the SE ones show a negative slope of the spectral ratio. Considering the positions of events 1 and 2, the effect of the attenuation of the interhypocentral medium on the spectral ratio would show the opposite pattern. Spectral-ratio variations of this doublet therefore can not be attributed to the effect of attenuation in the hypocentral zone. The spectral-ratio pattern reported for the S5 doublet is also incompatible with this effect.

On the other hand, even if the sign of the $G(f)$ variations was consistent with the effect of the attenuation between the two hypocentres, the amplitude of these variations is too strong to be attributed to this cause. Indeed, if we attribute the variations of spectral ratios to attenuation between the two hypocentres of a doublet, and if we assume that the radiation of the source $A_0(f)$ is the same for the two events, the spectral ratio $G(f)$ can be expressed:

$$G(f) = \exp\left(-\frac{\pi f t}{Q}\right) \tag{6}$$

where f is the frequency, t the traveltime between the two hypocentres, Q the quality factor. The mean slope of the logarithm of the spectral ratio can therefore be written:

$$a = -\frac{\pi d}{QV} \tag{7}$$

where d is the interevent distance, V the mean P- or S-wave velocity in the vicinity of the two foci.

For a distance between the foci of 50 to 100 m and a P-wave velocity of 5 to 8 km s^{-1}, the traveltime in the focal zone $t = d/V$ is about 0.01 s. As $|a|$ is about 0.01 s to 0.05 s, the corresponding Q value would be about one, which seems unrealistic, for most crustal material. Observed a slopes are one or two orders of magnitude too strong to be related to the attenuation process between the two hypocentres. As a conclusion, this method can not provide measurements of Q in the hypocentral region.

(b) Variation of the attenuation due to the occurrence of the first earthquake

Crustal attenuation may be altered within the focal zone, following the occurrence of the first event.

The main effect corresponds to the non-common part of

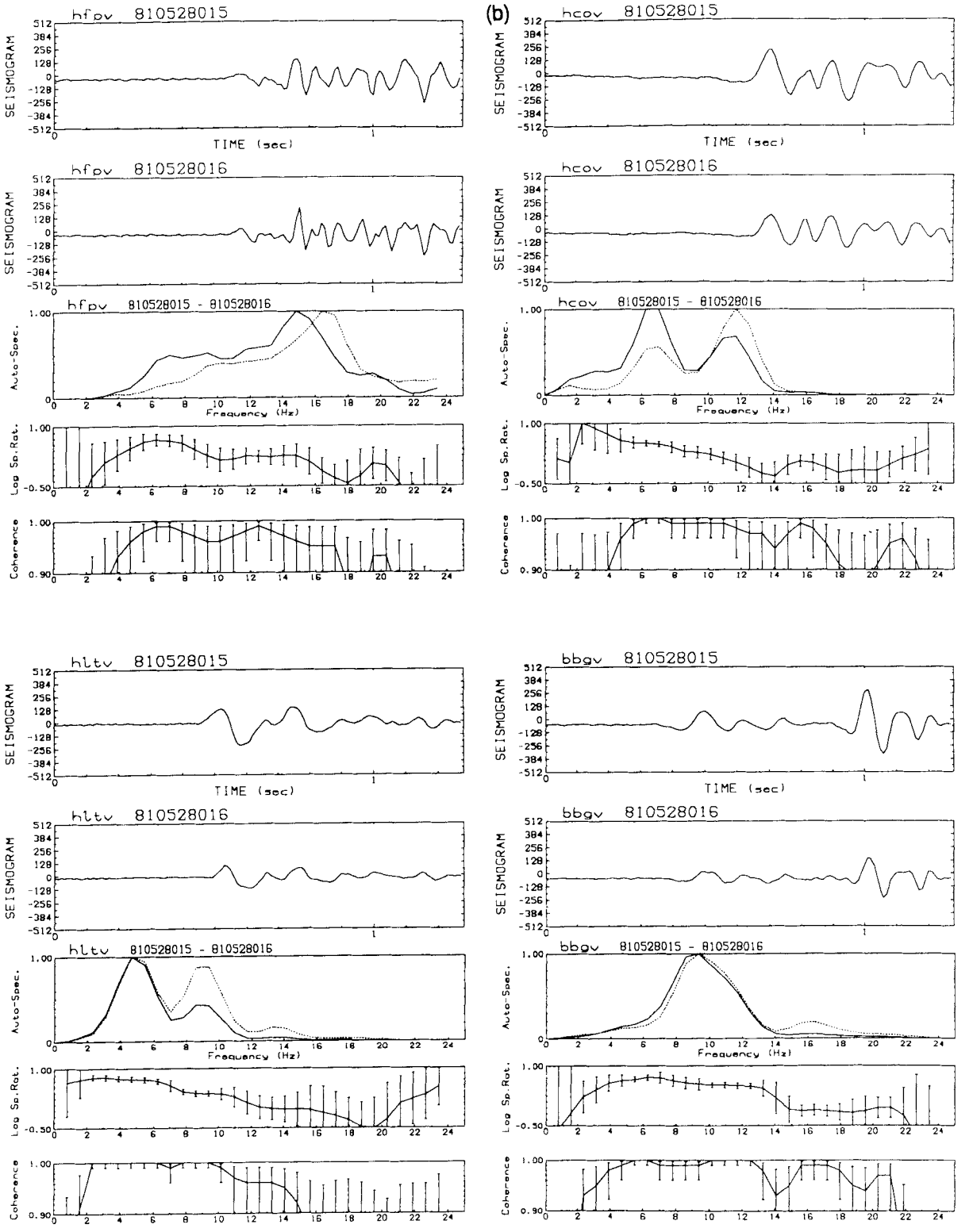

Figure 3. (*Continued.*)

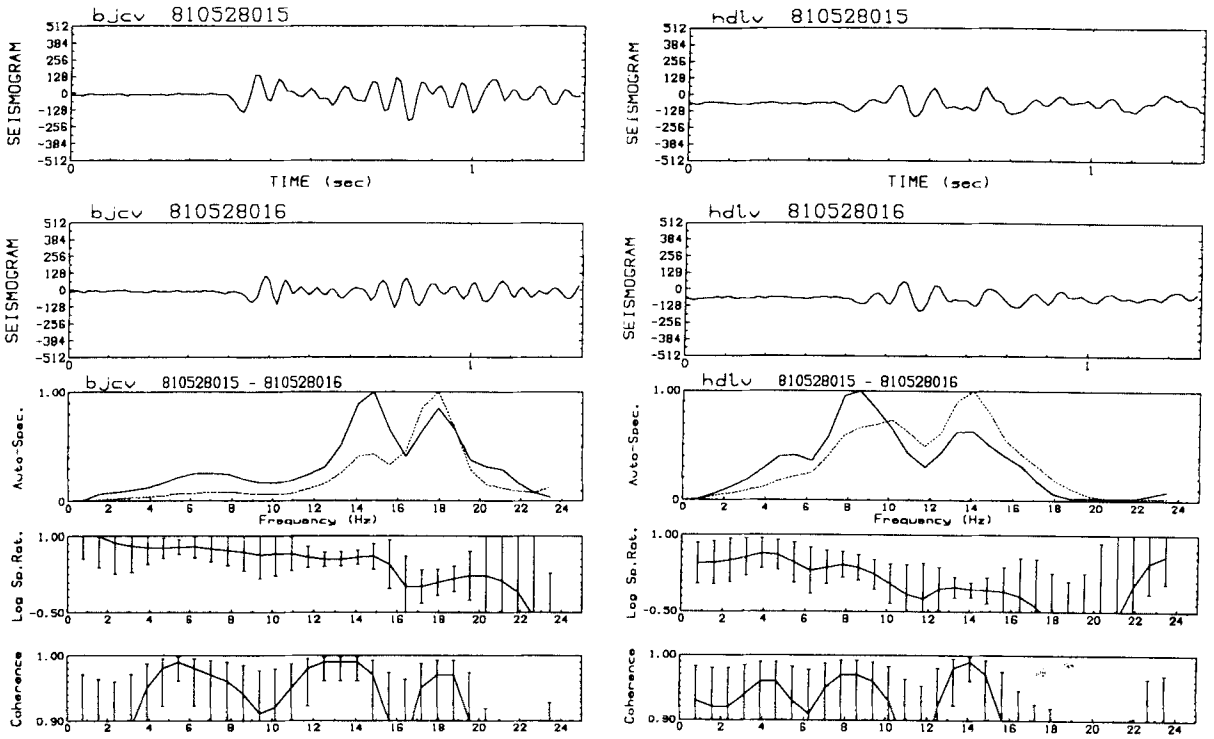

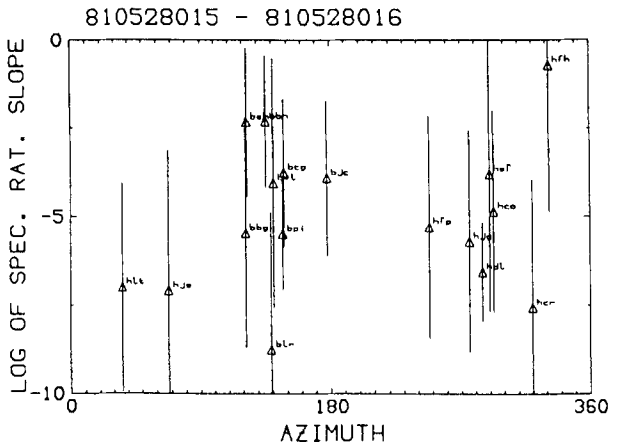

Figure 3(b). (*Continued.*)

the ray, inside the ellipsoid whose foci are the hypocentres of the two events. A change of attenuation in this ellipsoid would induce an asymmetry in the azimuthal variation of spectral ratios. This pattern is not observed.

Effect of source changes

The preceding discussion leads us to pay attention to the effect of the source. Also, in the following paragraphs, we will try to ascribe changes in spectral ratios to some pertinent earthquake source parameters. Following Aki & Richards (1980), for a kinematic source model, the far-field displacement waveforms of P waves propagating in an elastic, isotropic and homogeneous medium is described by

$$\mathbf{u}(\mathbf{x},t)=\frac{\mu}{4\pi\rho c^3 r}R\int\Delta\dot{u}(t-r/c)\,dS \qquad (8)$$

in the Fraunhofer approximation, where $\mathbf{x}$ is the position of the observer, t the time, μ and ρ are respectively the rigidity and the density of the propagating medium, c is the velocity of P waves, r is the distance between the observer and the source, R is the radiation pattern for P waves, and $\Delta\dot{u}$ the slip velocity. That is,

$$\mathbf{u}(\mathbf{x},t)=\frac{\mu}{4\pi\rho c^3 r}R\int_0^\tau\Delta\dot{u}\left(t-\frac{r}{c}\right)\dot{S}(t)\,dt \qquad (9)$$

Table 2. Distance in (km), azimuth and take-off angle (in degrees) for the S6 doublet. Closest stations were clipped and have been discarded.

Station	Distance	Azimuth	Take-off Angle
bcgv	18.3	125	91
hcbv	19.4	317	90
hcov	19.4	298	90
hltv	20.2	64	90
hfev	22.2	26	90
blrv	26.3	126	90
hgwv	26.7	332	90
hqrv	26.9	83	90
bjcv	30.4	159	90
hgsv	32.9	10	90
jrrv	33.8	325	90
jbzv	36.3	311	90
jcbv	37.6	335	74
bvlv	38.4	131	74
jrgv	47.9	303	74

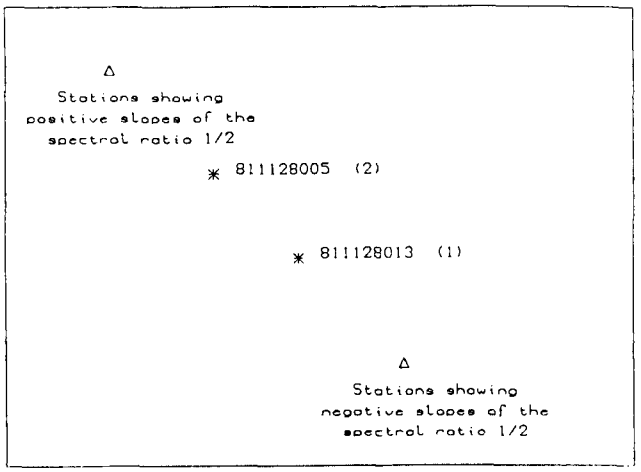

Figure 4. Schematic representation of the relative location for S6 doublet events (stars). The axis of this doublet is nearly horizontal.

where τ is the rupture time and $\dot{S}(t)$ is the velocity of increase of the isochrone area, as defined in Bernard & Madariaga (1984). So we can write

$$\mathbf{u}(\mathbf{x}, t) = \frac{\mu}{4\pi\rho c^3 r} R\, \Delta\dot{u}(t) * \dot{S}(t). \tag{10}$$

Therefore, the far-field displacement P pulse appears to be the velocity $\dot{S}(t)$ smoothed by the slip velocity. If the rise time is far lower than the rupture time, the slip velocity tends to be a Dirac function and the displacement pulse becomes merely proportional to $R\dot{S}(t)$. As a consequence, any change in the isochrones may induce a change in the displacement pulse, and then can produce a spectral ratio variation. Scherbaum & Wendler (1986) have already demonstrated that such variations lead to changes in phase of the transfer function.

However, any change in $\dot{S}(t)$ does not explain the azimuthal variations, especially their sign, observed in a slopes. As Scherbaum & Wendler (1986) emphasized for time delays, we have to consider a change in the radiation pattern, correlated with a change in the displacement pulse. Bakun, Stewart & Bufe (1978) also proposed such an explanation to account for difference in the high-frequency radiation of very similar earthquakes in Central California.

Isochrone variations leaving constant the rupture time act on frequencies higher than the corner frequency, and can probably explain the non-linearities observed on spectral ratios. However, they can not account for the corner-frequency shifts noticed in Fig. 3. We therefore will be interested by changes in average characteristics of the displacement pulse, in time and at first in frequency space.

(a) Relation between spectral ratio slope and change in source parameters

Aki & Richards (1980) describes the far field displacement spectrum $A(f)$ for kinematic fault models by:

$$A(f) = A_0 \frac{1}{\left[1 + \left(\frac{f}{f_c}\right)^p\right]^q} \tag{11}$$

where $A_0 = A(0)$ is proportional to the seismic moment, and f_c, the corner frequency, is proportional to the inverse of the fault length. p and q characterize the high-frequency asymptote and are related to the fault model. A source point corresponds to $(p, q) = (2, 3/2)$ (f^3 model). $(p, q) = (2, 1)$ (f^2 model) corresponds to a kinematic fault model for which stopping phases are dominant at high frequency. The average frequency changes in the spectral ratio, expressed by $\bar{G}_{LFm}$ and a, can therefore arise from:

—a variation of A_0: this variation is expressed by $\bar{G}_{LFm}$ and corresponds to a variation of seismic moment.

—a variation of f_c, which produces the variation:

$$\ln [G(f)] = q \ln \frac{1 + \left(\frac{f}{f_{c_2}}\right)^p}{1 + \left(\frac{f}{f_{c_1}}\right)^p}. \tag{12}$$

$\ln G(f)$ varies with frequency as shown in Fig. 5 for the f^2 model. Although $\ln G(f)$ is not a linear function of f, note that it is close to a straight line for a small frequency shift between the two spectra.

We now search for a simple relation between the average slope a of $\ln G(f)$ and a significant physical source parameter. Let us remark that, since the coherency is generally higher than 0.90 in a frequency band roughly centred on the corner frequency $f_c \approx f_{c_1} \approx f_{c_2}$ (about 10 Hz), the computed a slope corresponds to an average rate of change of $\ln G(f)$ around f_c. In the vicinity of $f = f_c$, the first order variation of $\ln G(f)$ is

$$\begin{aligned} a(f = f_c) &= \left[\frac{d}{df} \ln G(f)\right](f = f_c) \\ &= pqf_c^{p-1} \frac{f_{c_1}^p - f_{c_2}^p}{(f_{c_2}^p + f_c^p)(f_{c_1}^p + f_c^p)} \\ &= \frac{pq}{4} f_c^{-(p+1)} (f_{c_1}^p - f_{c_2}^p) \quad \text{as} \quad f_c \approx f_{c_1} \approx f_{c_2}. \end{aligned} \tag{13}$$

In order to estimate the dependence on the model, we could write $a(f_c) = -q\,\Delta f_c / f_c^2$ since $p = 2$ for both models, $f_c \approx f_{c_1} \approx f_{c_2}$ and $\Delta f_c = f_{c_2} - f_{c_1}$. It appears that there is no dramatic dependence of $a(f_c)$ on the model. In the following, we will use Aki's f^2 model and shortly note $a(f_c)$ as a so that we have

$$a = -\frac{\Delta f_c}{f_c^2}. \tag{14}$$

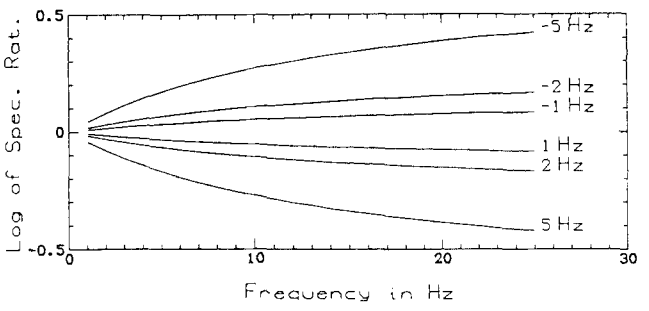

Figure 5. Logarithm of spectral ratio versus frequency for different (−5 Hz to 5 Hz) corner frequency changes using Aki's ω-square model of spectrum.

This relation demonstrates that the slope of $\ln G(f)$ is expected to be proportional and opposite to the variation of corner frequency, as it is observed (Fig. 3). Note also that frequency shifts and a slopes are stronger for S5 doublet than for S6 one. For a corner frequency $f_c \approx 10$ Hz, and for $\Delta f_c \approx 1$ Hz, the order of magnitude of a (0.01 s) corresponds to the observed variations.

Assuming that the rise time is much smaller than the rupture duration, we can equate the corner frequency to the reciprocal of the rupture duration τ. Therefore the a slope of $\ln G(f)$ computed in the vicinity of f_c is an indirect estimation of the variation in the apparent rupture duration $\Delta\tau$:

$$a = \Delta\tau. \tag{15}$$

As a result, the variation in apparent rupture duration is about $0.02\text{ s} \pm 0.01\text{ s}$ for the stations located in the fault azimuth of the S6 doublet, and $0.05\text{ s} \pm 0.02\text{ s}$ for the S5 doublet.

(b) Possible origins for rupture duration changes

In the Fraunhofer approximation, the Haskell's rectangular fault model (Aki & Richards 1980) allows us to write a simple relation for τ:

$$\tau = \frac{L}{v_r}\left(1 - \frac{v_r}{c}\sin\phi\cos\theta\right) \tag{16}$$

where L is the fault length, v_r the rupture velocity, $c = v_p$ or v_s the P- or S-wave velocity, θ is the azimuth of the station relative to the rupture direction, and ϕ is the take-off angle.

The range of take-off angles is very narrow and does not allow us to observe spectral-ratio variations with the take-off angle, in a given azimuth. Nevertheless, it is likely that such variations exist, although we are unable to show evidence of them. Since the take-off angle ϕ is close to 90° for the most part of the stations used (Table 2), we merely use τ for $\phi = 90°$:

$$\tau = \frac{L}{v_r}\left(1 - \frac{v_r}{c}\cos\theta\right). \tag{17}$$

Therefore a change of rupture duration can be ascribed to a focal mechanism variation, a change in the average rupture velocity v_r, or a change in the geometry of the source (variation in dimension, or in the position of the hypocentre).

(1) *Focal mechanism changes.* For a doublet, the variation in focal mechanism is small (otherwise, the two events can not constitute a doublet). Let us consider such a small change $\Delta\theta$ in fault-plane orientation. The corresponding variation of apparent rupture duration, computed from eq. (17) is:

$$\Delta\tau = \frac{L}{c}\sin\theta\Delta\theta. \tag{18}$$

According to that assumption, $\Delta\tau$ would be null in the fault azimuth, and maximum for $\theta = \pi/2$. Fig. 3(a) clearly reports the opposite pattern. Hence, such a change in focal mechanism does not explain correctly the measured $\Delta\tau$.

(2) *Rupture velocity variation.* Such a variation induces a change $\Delta\tau = -(L/v_r^2)\,\Delta v_r$ in apparent rupture duration. Note that the resulting change of τ has the same value for all azimuths, and therefore is unable to explain azimuthal variations of τ.

(3) *Change in source dimension.* A change in fault length leads to a variation of τ:

$$\Delta\tau = \frac{\Delta L}{v_r}\left(1 - \frac{v_r}{c}\cos\theta\right). \tag{19}$$

If the source dimension varies, the sign of ΔL does not depend on θ, and $1 - (v_r/c)\cos\theta$ is positive regardless of θ as long as $v_r < c$. $\Delta\tau$ therefore has the same sign for all azimuths. Such a change in source dimension does not explain the spectral changes observed on the S6 doublet, but it is the most likely explanation of those reported for the S5 doublet. Indeed this doublet exhibits at the same time strong positive-spectra shifts and negative a slopes for all azimuths, and a large variation of seismic moment between the two events, as expected from a source dimension variation. Note that both $\Delta\tau$ and seismic-moment variation are about twice as large as for S5 as for S6. A change ΔL of about 50 per cent in the total length L is necessary to explain the spectral changes observed on S5 doublet.

(4) *Change in the position of the hypocentre.* The former discussion proves that S6 azimuthal distribution of $\Delta\tau$ is not explained by changes in focal mechanism, rupture velocity or fault dimensions. Let us now consider the effect of a change in the position of the hypocentre relative to the fault plane: in that case, the rupture process is assumed to be a bilateral one. Bilateral faulting induces variations of the same type as unilateral faulting, for changes in focal mechanism, rupture velocity or fault dimensions.

We will use simple geometrical assumptions to derive a relation between $\Delta\tau$ and hypocentre location. Assuming a bilateral rupture on a rectangular area, we can make two different hypotheses to calculate τ: either τ is the difference between the initiating phase and the latest stopping phase (a), or τ is the difference the two stopping phases (b). τ can be expressed as follows:

$$\begin{cases} \tau = \dfrac{l}{v_r}\left(1 + \dfrac{v_r}{c}\cos\theta\right) & -\theta_l \le \theta \le \theta_l \\ \tau = \dfrac{L-l}{v_r}\left(1 - \dfrac{v_r}{c}\cos\theta\right) & \theta_l \le \theta \le 2\pi - \theta_l \end{cases} \tag{20a}$$

$$\begin{cases} \tau = \dfrac{2l}{v_r} - \dfrac{L}{v_r}\left(1 - \dfrac{v_r}{c}\cos\theta\right) & -\theta_l \le \theta \le \theta_l \\ \tau = -\dfrac{2l}{v_r} + \dfrac{L}{v_r}\left(1 - \dfrac{v_r}{c}\cos\theta\right) & \theta_l \le \theta \le 2\pi - \theta_l \end{cases} \tag{20b}$$

where L is the fault length, and l the distance between the border of the rectangular fault and the hypocentre.

$$\theta_l = \cos^{-1}\left[\frac{c}{v_r}\left(1 - \frac{2l}{L}\right)\right]$$

does not exist if

$$0 \le l < \frac{L}{2}\left(1 - \frac{v_r}{c}\right) \quad \text{or} \quad \frac{L}{2}\left(1 + \frac{v_r}{c}\right) < l \le L.$$

In that case, τ keeps the same expression for all azimuths and the rupture can be considered as a quasi-unilateral rupture. As a consequence, a change in the position of the hypocentre relative to the rupture area would act as a change in fault length.

In the 'central zone' of the rupture area

$$\left[\frac{L}{2}\left(1-\frac{v_r}{c}\right)\leq l\leq\frac{L}{2}\left(1+\frac{v_r}{c}\right)\right]$$

a small change Δl in the position of the hypocentre produces the following variation of τ:

$$\begin{cases}\Delta\tau=\dfrac{\Delta l}{v_r}\left(1+\dfrac{v_r}{c}\cos\theta\right) & -\theta_l\leq\theta\leq\theta_l\\ \Delta\tau=-\dfrac{\Delta l}{v_r}\left(1-\dfrac{v_r}{c}\cos\theta\right) & \theta_l\leq\theta\leq 2\pi-\theta_l\end{cases}\qquad(21a)$$

$$\begin{cases}\Delta\tau=2\dfrac{\Delta l}{v_r} & -\theta_l\leq\theta\leq\theta_l\\ \Delta\tau=-2\dfrac{\Delta l}{v_r} & \theta_l\leq\theta\leq 2\pi-\theta_l\end{cases}\qquad(21b)$$

$\Delta\tau$ therefore has opposite signs in opposite directions in both relations (21a) and (21b). This result is in agreement with the azimuthal pattern of $\Delta\tau$ reported for the S6 doublet. From the later relation, we can see that a variation Δl that produces a change $\Delta\tau\approx 0.02$ s is of the order of 30 m, that is, about 30 per cent of the total length L.

Delocation of hypocentres is only the simplest explanation concerning a-slopes variations. In the framework of a bilateral rupture, other differences in source process—especially in the way the rupture propagates and stops—can account for our observations. However, it highlights that even microearthquakes of weak magnitude can have a relatively complex rupture process.

In order to check our hypotheses concerning the origin of a slopes, we have performed a numerical simulation of bilateral ruptures, for which hypocentres locations may vary on the rupture area. In this aim we have used the Discrete Wavenumber method to compute synthetic seismograms (Bouchon 1981), corresponding to each event of the doublet. We consider a vertical strike-slip fault of rectangular (100 m × 50 m) shape, represented by a rectangular distribution of 10 × 5 double couples. The rupture initiates on the fault plane and propagates bilaterally with a constant velocity $v_r = 2.6\ \mathrm{km\,s^{-1}}$ (corresponding to $0.75v_s$). The source-time function used is a ramp with a rise time of 0.01 s. We used a simple velocity model for the layered crust, derived from a study by Blümling, Mooney & Lee (1985) (Table 3). The depth of the hypocentre is 5 km. For each doublet, we ran two computations for faults having different lengths, different rupture velocity or different hypocentres. The hypocentres belong to the 'central zone' of the fault. The synthetic seismograms are computed for 12 stations located at different azimuths but at the same distance (10 km). These seismograms are then considered like the records of a doublet, and their spectral ratios are computed using the Cross-Spectral Moving-Window Technique.

Table 3. Velocity model for the Calaveras Fault zone (From Blümling *et al.* 1985).

Depth (km)	v_p (km/s)	v_s (km/s)
4.0	4.5	2.6
13.0	6.0	3.4
16.5	7.0	4.1

Different fault lengths or rupture velocities do not provide positive and negative slopes of the spectral ratio, as it was inferred by our previous calculations. On the other hand, different hypocentres produce positive and negative spectral ratio slopes (Fig. 6) with an azimuthal organization similar to that observed in our data. Fig. 6 shows that a difference in hypocentre position relative to the borders of the rupture zone, of about 10 m is sufficient to explain variations of spectral ratio observed for S6 doublet. This means that very small differences of rupture kinematics can be responsible for observable variations of the spectral ratio of doublets.

It is interesting to remark how the changes we observed for S6 doublet are comparable to those pointed out by Bakun *et al.* (1978), although they are an order of magnitude smaller. These authors studied two events of magnitude 2.8 and 3.0 sharing the same location and the same focal mechanism on the San Andreas fault in Central California, that occurred within 5 min of one another. They noticed a remarkable change in the frequency content of P waves between both earthquakes, showing an azimuthal distribution of changes in the frequency content of the spectra. These results were interpreted as the effect of opposite directions of rupture propagation for each event. Although the scale of the two phenomena is not the same, Bakun's and our conclusions are not mutually exclusive.

IMPLICATIONS FOR TIME VARIATIONS OF CODA AMPLITUDES

Fig. 7 shows the evolution of a slopes, and consequently of the variation in apparent rupture duration $\Delta\tau$, from the P first arrivals until the end of the coda. They have been computed with a weighted least-squares adjustment, the weight used being similar to (5). The a slopes and their 90 per cent confidence intervals are plotted if the weighted mean coherency (estimated using the later weight) is greater than 0.90. From the S6 doublet (Fig. 7a), different observations can be reported. Although there is a smoothing effect due to the width of the time window, P and S first arrivals are clearly marked by strong absolute values of $\Delta\tau$. Remarkably, for stations where $\Delta\tau$ values are strong enough in the first arrivals to be distinguished from their value in the coda, it is possible to correlate S first arrivals with onsets of $\Delta\tau$. For the most part of the stations recording the S6 doublet, the absolute value of $a=\Delta\tau$ tends to decrease in the coda. For stations showing positive $\Delta\tau$ in the first arrivals (e.g. HGWV), $\Delta\tau$ decreases in the coda, and conversely (e.g. HLTV). To better describe the average decrease of $|a|=|\Delta\tau|$ in the coda for the whole set of stations, we have defined a_t as the time gradient of a_S, the slope in $\ln G(f)$ for S waves. The plot of a_t versus a_S (Fig. 8), shows that the time variation of $\Delta\tau$ is strongly correlated to the sign of its first arrivals value. Fig. 3(a) (bottom) shows that the variation of apparent rupture duration $\Delta\tau$

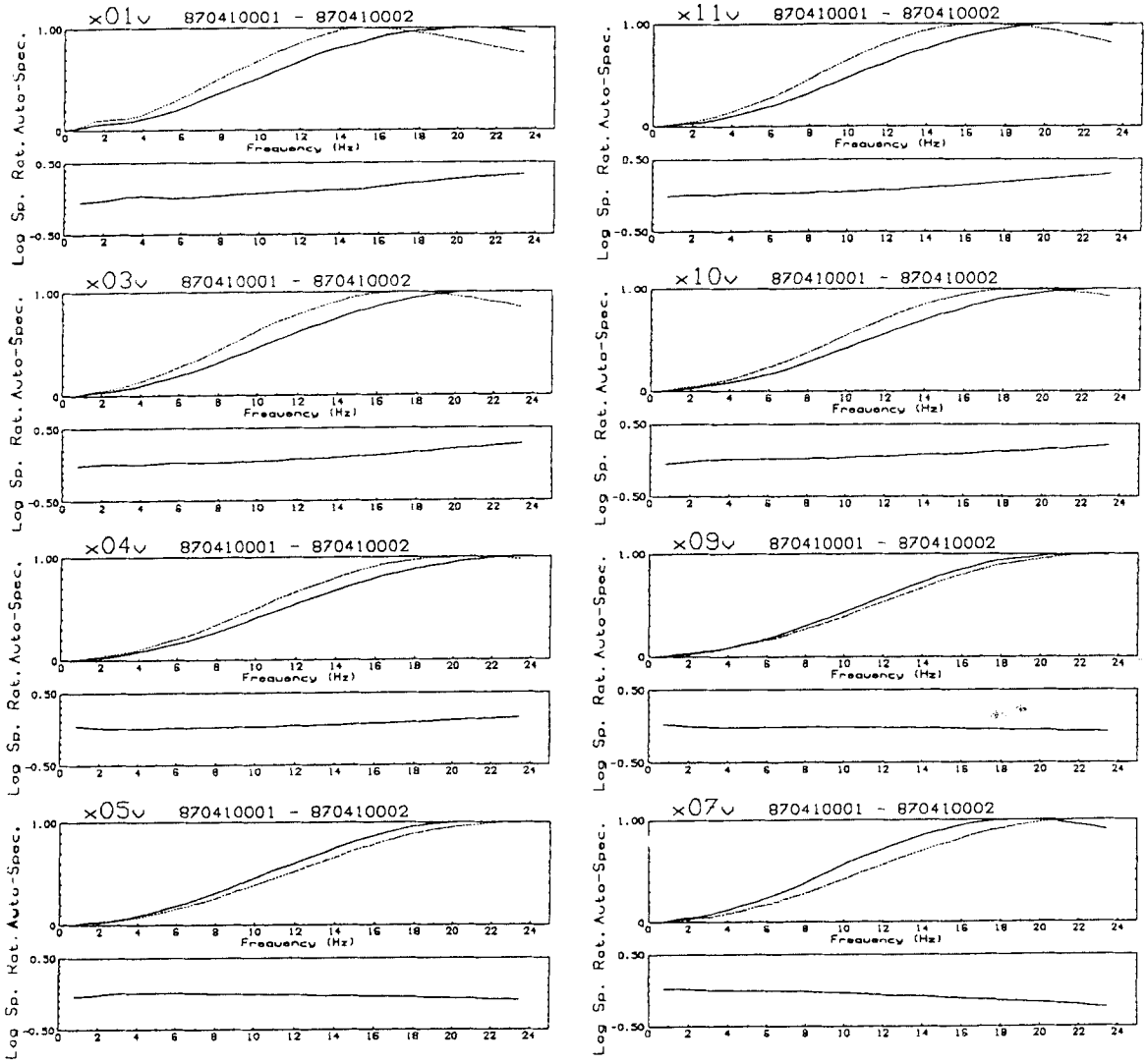

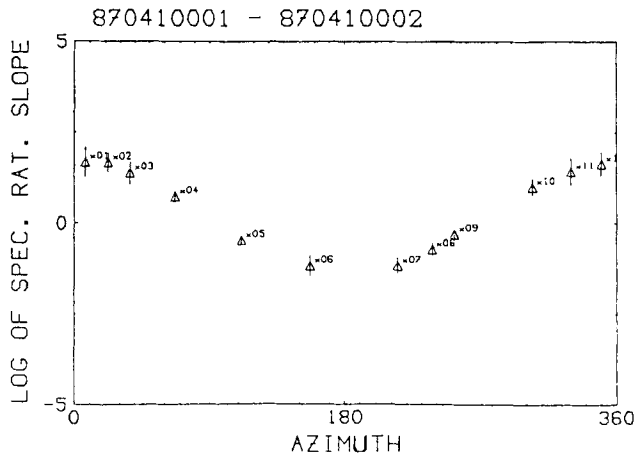

Figure 6. Logarithm of *P*-waves spectral ratio and autospectra for synthetic signals originating from sources having different hypocentres ($l = 45$ m for the first event and $l = 55$ m for the second event). Bottom: slopes of *P*-waves spectral-ratio logarithm × 100 as a function of azimuth for the synthetic seismograms. Triangles indicate different stations.

characterized the azimuth of the first-arrival wavetrains: so $\Delta\tau$ can be considered as a marker of the azimuth for each wave train. $|\Delta\tau|$ is maximum in the fault azimuth, and minimum along the normal to the fault trace for the S6 doublet (Fig. 3a). A similar pattern can not be discarded for the take-off angle distribution of $|\Delta\tau|$, although the narrow range of take-off angle does not allow us to observe it. Also, the average decrease of $|\Delta\tau|$ in the coda can be interpreted as an evidence that the later parts in the seismograms of microearthquakes recorded along the San Andreas fault, are waves leaving the source with increasing azimuths or take-off angles. Coda waves coming from increasing azimuths can be understood as an effect of the strong lateral refractions and reflections along the San Andreas fault. A closeby conclusion has been previously reached by Fréchet (1985), from time-delay measurements in the coda of spatial doublets: they provide a similar pattern to that observed for the spectral ratios (Fig. 9).

The time decrease of $|\Delta\tau|$ in the coda of a spatial doublet implies that there are measurable variations of corner frequency and spectral amplitudes in the coda that are not related to the attenuation process. This result is in

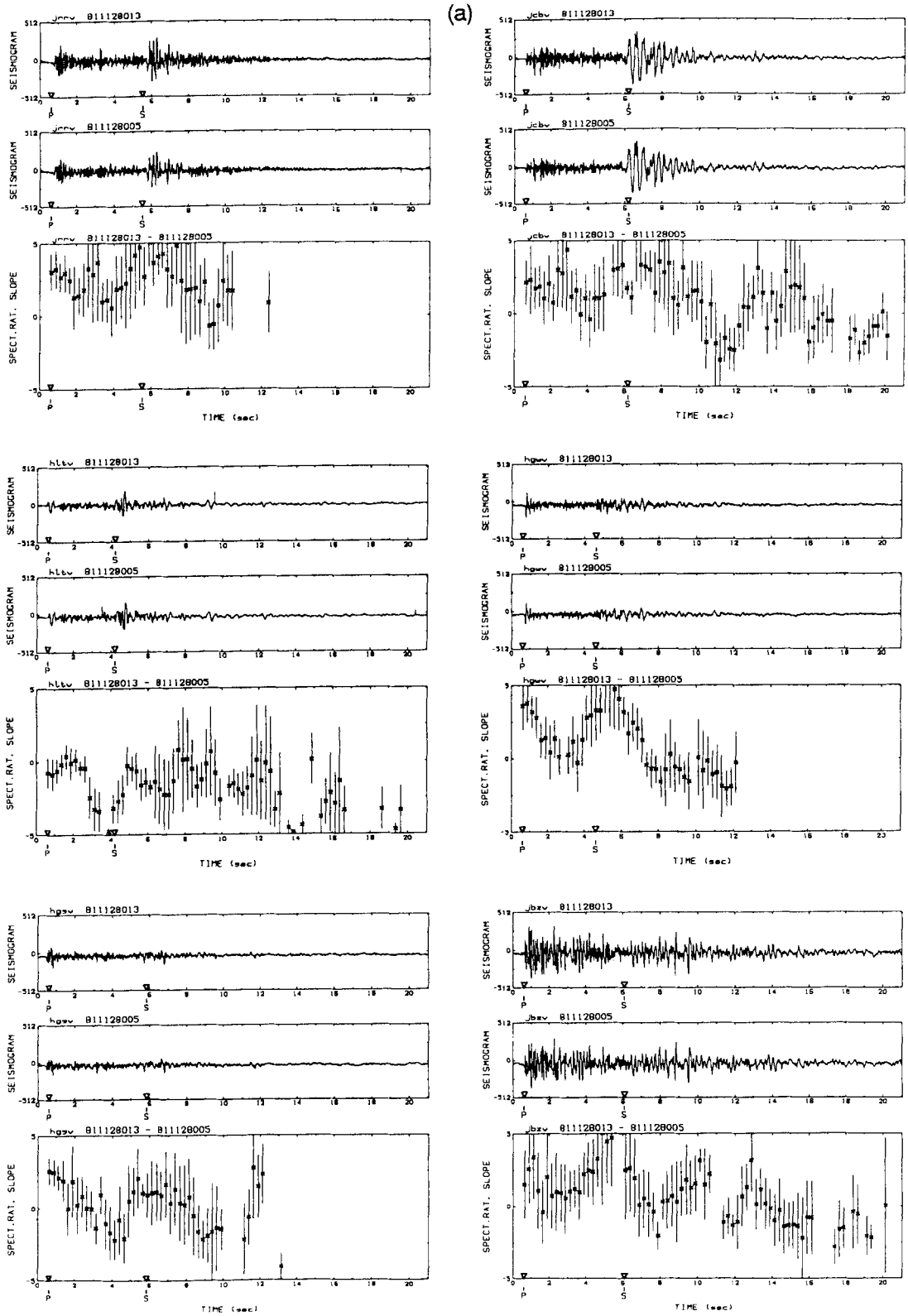

Figure 7. Variation of the slope of the spectral-ratio logarithm (or variation of apparent rupture duration) along the seismograms of S6 (a) and S5 (b) doublets. Vertical bars indicate 90 per cent confidence intervals.

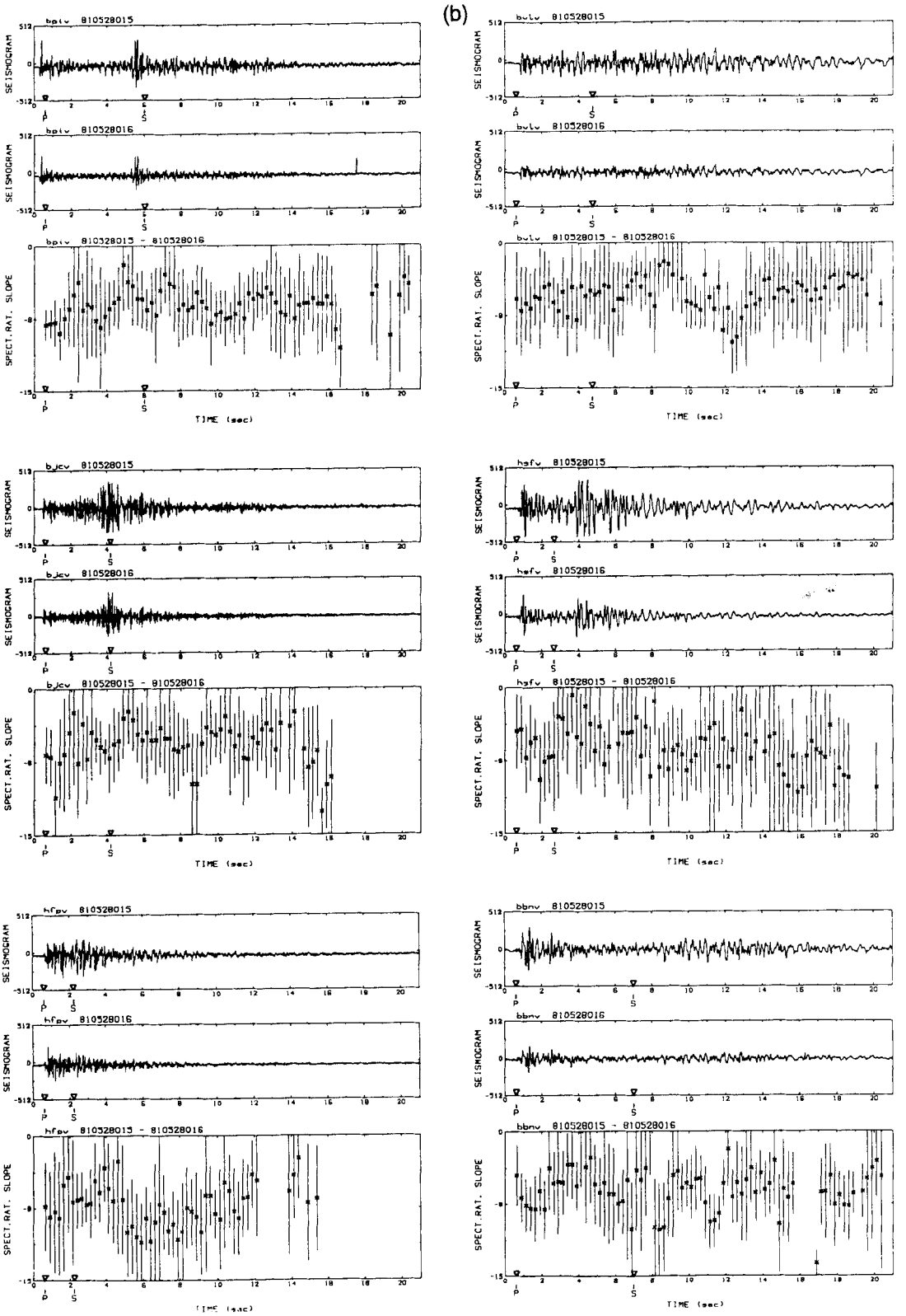

Figure 7. (*Continued.*)

agreement with Sato's (1984), who reports that the shape of early coda amplitudes is strongly affected by the fault plane solution. Coda-amplitude variations similar to S6 doublet ones have been clearly observed on temporal doublets, and are related to an azimuthal pattern of a slopes close to the one presented in Fig. 3 (Got *et al.* 1990). These changes have the same magnitude than those provoked by a temporal variation of the attenuation of 10 per cent. This incites to be very careful when dealing with temporal changes in coda Q^{-1}. To compare Q^{-1} values for different

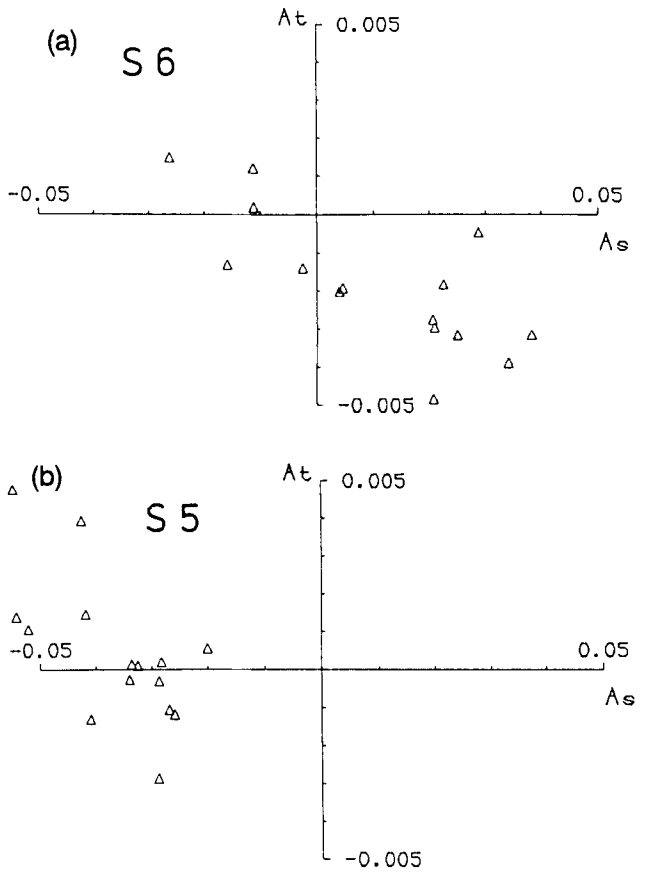

Figure 8. Slope of time decay of spectral-ratio logarithm a_t, versus slope of spectral-ratio logarithm in S waves for S6 and S5 doublets.

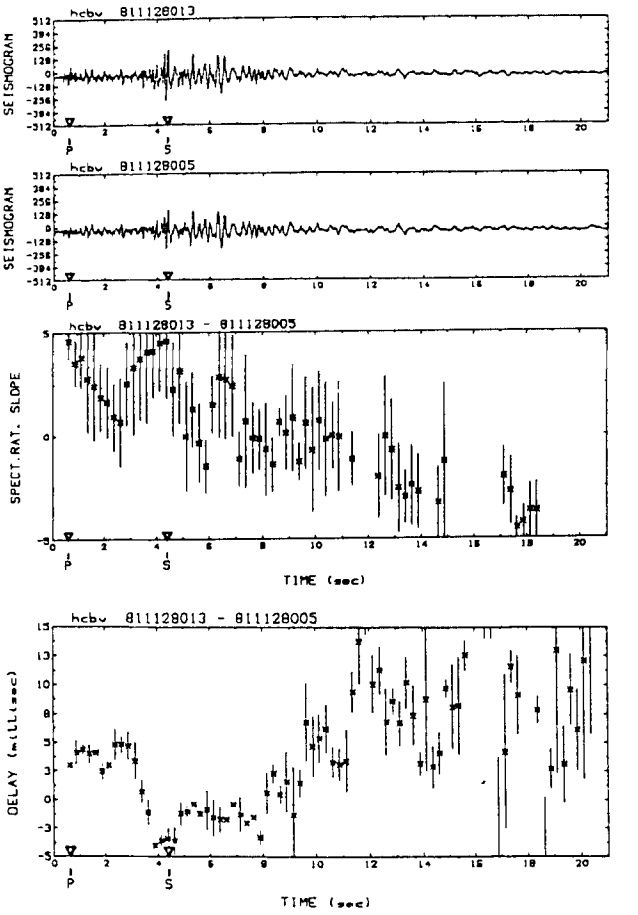

Figure 9. Slope of the spectral-ratio logarithm (or variation of apparent-rupture duration, in hundredth of seconds) and delay (in milliseconds) versus time for the station HCBV of S6 doublet. The absolute value of the two quantities shows a time decrease in the coda.

periods, we propose to pay special attention to the number and the distribution of locations and focal mechanisms within the set of earthquakes used. Indeed, as Frankel (1991) emphasized, numerous coda-Q^{-1} studies used the relatively early coda, with lapse times less than twice the traveltime of the direct S wave. Furthermore, it is precisely this part of the coda that may contain information on an incoming shallow earthquake, in near stations. It is very likely that the effect of focal mechanism changes in the early coda can be far stronger when comparing very different earthquakes rather than doublets. Such an effect could be partly responsible for the complicated and various patterns of changes in measured coda Q^{-1}.

Another interesting feature (Fig. 7a) is that the general decrease of $|\Delta\tau|$ in the coda is sometimes perturbated in some parts of the coda (see for example stations JCBV, JBZV, HGSV). The wave trains which arrive at this time in the coda can be deep reflections or surface waves propagating in the superficial layers below the station.

For the S5 doublet, time variations of $\Delta\tau$ are different from those observed previously (Fig. 7b). The a slopes for S5 are strongly negative (notice the change in ordinates between Figs 7a and b) and they keep approximately the same value all along the seismograms, having regard to the large confidence intervals due to the poor linear fit of $\ln G(f)$ for this doublet. However, the relative constancy of $a = \Delta\tau$ in the coda can be related with its value in the first arrivals. In fact, Fig. 8(b) points out that all stations are located in the a_s-negative half-space, with a weak correlation between a_S and a_t. As a consequence, it does not contradict the former interpretation on the origin of $\Delta\tau$ time variations: in that case $\Delta\tau$ is not as good marker of the azimuth as it was for the S6 doublet, and the reason has to be found in the different source processes.

CONCLUSION

Two spatial doublets from Central California have been studied using Cross-Spectral Moving-Window Technique. Although both events of each doublet occur very closely in time, spectral-ratios exhibit steady variations in the first arrivals and in the coda. The patterns of these variations allow us to discard unambiguously the possibility of amplitude changes related to attenuation process between the hypocentres. Therefore this method can be used to compute, neither Q in the focal zone, nor time variations of Q^{-1} using temporal doublets. On the contrary, the average rate of spectral-ratio changes, accurately estimated when the coherency is greater than 0.90 on large bandwidths, is clearly related to the variation of apparent rupture duration and provides an indirect measure of it. As a consequence, the

physical parameters which control the average linear trend in frequency variations of spectral ratio computed in the first arrivals of doublets are the fault length and the hypocentre location relative to the rupture area. A change of about 50 per cent in source dimensions explains the amplitude variations computed for the S5 doublet. On the other hand, different positions of the hypocentres relative to the borders of their respective rupture area account for the positive and negative variation in apparent rupture durations reported for the S6 doublet. It shows that microearthquakes can have complex rupture processes, involving bilateral or circular propagation. The computed delocation between the hypocentres is of the order of 10 to 30 per cent of the source length. These relatively weak changes in source geometry and kinematics produce not only measurable amplitude variations in the first arrivals, but also different time changes in the amplitudes of coda waves. As a matter of fact, several stations of the S6 doublet have weaker and weaker spectral-ratio variations (and therefore variations of apparent rupture duration) with the elapsing time in the coda. The S5 doublet, for which the sign of variation in apparent rupture durations is not azimuthally dependent, displays the opposite pattern with spectral-ratio variation (and variation of apparent rupture durations) identical all along the coda. The arrival in the coda of waves leaving the source with increasing azimuths (or take-off angles), likely due to the strong lateral refraction reported along the San Andreas Fault, is the most probable explanation of these observations. Although this effect could be only a local one, it could corrupt the measure of changes in coda Q^{-1} from temporal doublets, and likely from usual microearthquake studies. It suggests that the interpretation of coda amplitude ratios in small-magnitude microearthquakes doublets, and *a fortiori* of coda-decay changes for very different earthquakes, as Q^{-1} temporal changes have to be carried out very carefully.

ACKNOWLEDGMENTS

We are grateful to M. Bouchon, who provided the program allowing the computation of synthetic seismograms. We thank F. J. Chavez-Garcia and both anonymous reviewers for their numerous suggestions which improved our manuscript.

REFERENCES

Aki, K. & Richards, P. G., 1980. *Quantitative Seismology: Theory and Methods*, W. H. Freeman, San Francisco.

Aki, K., 1985. Theory of earthquake prediction with special references to monitoring of the quality factor of lithosphere by coda method, *Earthq. Pred. Res.*, **3,** 219–230.

Aster, R., Shearer, P. & Berger, P., 1990. Quantitative measurements of shear-wave polarizations at the Anza seismic network, southern California—implications for shear-wave splitting and earthquake prediction. *J. geophys. Res.*, **95,** 12449–12474.

Bakun, W. H., Stewart, R. M. & Bufe, C. G., 1978. Directivity in the high-frequency radiation of small earthquakes, *Bull. seism. Soc. Am.*, **68,** 1253–1263.

Bernard, P. & Madariaga, R., 1984. A new asymptotic method for the modeling of near-field accelerograms, *Bull. seism. Soc. Am.*, **74,** 539–557.

Blümling, P., Mooney, M. & Lee, W. H. K., 1985. Crustal structure of the southern Calaveras fault zone, Central California, from seismic refraction investigation, *Bull. seism. Soc. Am.*, **75,** 193–209.

Bouchon, M., 1981. A simple method to calculate Green's functions for elastic layered media, *Bull. seism. Soc. Am.* **71,** 959–971.

Chouet, B., 1979. Temporal variation in the attenuation of earthquake coda near Stone Canyon, California, *Geophys. Res. Lett.*, **6,** 143–146.

Crampin, S., Booth, D., Evans, R., Peacock, S. & Fletcher, J., 1990. Changes in shear-wave splitting at Anza near the time of the North Palm Springs earthquake, *J. geophys. Res.*, **95,** 11197–11212.

Frankel, A., 1991. Review 7A.4, *Evaluation of proposed earthquake precursors*, ed. Wyss, M., Am. geophys. Un., Washington, DC.

Fréchet, J., 1985. Sismogenès et doublets sismiques, *Thèse d'Etat*, Univ. sci. technol. médic., Grenoble.

Frémont, M.-J. & Poupinet, G., 1987. Temporal variation of body-wave attenuation using earthquake doublets, *Geophys. J. R. astr. Soc.*, **90,** 503–520.

Got, J.-L., Poupinet, G. & Fréchet, J., 1990. Changes in source and site effects compared to coda Q^{-1} temporal variations using microearthquake doublets in California, *Pure appl. Geophys.*, **134,** 195–228.

Gusev, A. A. & U. K. Lemzikov, 1985. Properties of scattered elastic waves in the lithosphere of Kamchatka: parameters and temporal variations, *Tectonophysics*, **112,** 137–153.

Jenkins, G. M. & Watts, D. G., 1968. *Spectral Analysis and its Applications*, Holden-Day, San Francisco.

Jin, A. & Aki, K., 1986. Temporal change in coda Q before the Tangshan earthquake of 1976 and the Haicheng earthquake of 1975, *J. Geophys. Res.*, **91,** 665–673.

Jin, A. & Aki, K., 1989. Spatial and temporal correlation between coda Q^{-1} and seismicity, and its physical mechanism, *J. geophys. Res.*, **94,** 14041–14059.

Novelo-Casanova, D. A., Berg, E., Hsü, V. & Helsley, E., 1985. Time-space variations of seismic S-wave coda attenuation Q^{-1} and magnitude distribution (b-value) for the Petatlan earthquake, *Geophys. Res. Lett.*, **12,** 789–792.

Peacock, S., Crampin, C., Booth, D. & Fletcher, J., 1988. Shear-wave splitting in the Anza seismic gap, Southern California: temporal variations as possible precursors, *J. geophys. Res.*, **93,** 3339–3356.

Peng, J. Y., Aki, K., Lee, W. H. K., Chouet, B., Johnson, P., Marks, S., Newberry, J. T., Ryall, A. S., Stewart, S. W. & Tottingham, D. M., 1987. Temporal change in coda Q associated with 1984 Round Valley earthquake in California, *J. geophys. Res.*, **92,** 3507–3526.

Poupinet, G., Ellsworth, W. L. & Fréchet, J., 1984. Monitoring velocity variations in the crust using earthquake doublets: an application to the Calaveras fault, California, *J. geophys. Res.*, **89,** 5719–5731.

Sato, H., 1984. Attenuation and envelope formation of three-component seismograms of small local earthquakes in randomly inhomogeneous lithosphere, *J. geophys. Res.*, **89,** 1221–1241.

Sato, H., 1986. Temporal change in attenuation intensity before and after the eastern Yamanashi earthquake of 1983 in central Japan, *J. geophys. Res.*, **91,** 2049–2061.

Sato, H., 1988. Temporal change in scattering and attenuation associated with the earthquake occurence—a review of recent studies on coda waves, *Pure appl. Geophys.*, **126,** 465–497.

Scherbaum, F. & Wendler, J., 1986. Cross spectral analysis of Swabian Jura (SE Germany) three-component micro-earthquake recordings, *J. Geophys.*, **60,** 157–166.